THERE AND SHARP AGAIN: THE CIRCLE JOURNEY OF NUCLEONS AND ENERGY DEPOSITION*

Giuliano Giacalone

Institut für Theoretische Physik, Philosophenweg 16, 69120 Heidelberg, Germany

Received 13 August 2022, accepted 18 September 2022, published online 14 December 2022

A central question in high-energy nuclear phenomenology is how the geometry of the quark–gluon plasma (QGP) formed in relativistic nuclear collisions is precisely shaped. In our understanding of such processes, two features are especially crucial for the determination of the QGP geometry, respectively, the nucleon size and the energy deposition scheme. This contribution reports on the (circular) evolution of such features in state-of-the-art model incarnations of heavy-ion collisions over the past seven years. Ideas for future directions of investigation are pointed out.

DOI:10.5506/APhysPolBSupp.16.1-A10

1. Nucleon (or sub-nucleon) size and energy deposition

In the state-of-the-art picture of a heavy-ion collision, the interaction process acts as a quantum measurement for the transverse positions of the constituents of the colliding nuclei. A nucleus, say A, viewed in the laboratory frame is associated with a two-dimensional profile representing a snapshot of its content in the plane $\boldsymbol{x} = (x, y)$ at the time of interaction

$$T_A(\boldsymbol{x}) = \sum_{j=1}^{A_A} \lambda_j g(\boldsymbol{x}; \boldsymbol{x}_j w) \,, \qquad g(\boldsymbol{x}; \boldsymbol{x}_j w) = \frac{1}{2\pi w^2} \exp\left(-\frac{(\boldsymbol{x} - \boldsymbol{x}_j)^2}{2w^2} \right) \,, \tag{1}$$

where j labels the A_A nucleons in nucleus A, λ_j is a fluctuation associated with nucleon j, and $g(\boldsymbol{x}; \boldsymbol{x}_j, w)$ is the nucleon profile, commonly taken as a Gaussian, where $\boldsymbol{x}_j$ represents the center position of j and w is the anticipated nucleon size. What is the appropriate size for high-energy scattering? In DIS at low x, the dipole cross section at a given impact parameter is of the form of $\frac{\mathrm{d}\sigma_{q\bar{q}}}{\mathrm{d}^2\boldsymbol{b}} \propto r^2 \alpha_{\mathrm{s}} x g(\mu^2, x) T(\boldsymbol{b})$, where $T(\boldsymbol{b})$ weights the gluon density depending on the distance from the target's center. Diffractive production

* Presented at the 29th International Conference on Ultrarelativistic Nucleus–Nucleus Collisions: Quark Matter 2022, Kraków, Poland, 4–10 April, 2022.

of J/Ψ at HERA suggests that $T(\boldsymbol{b})$ can be modeled as a 2D Gaussian with width 0.35 fm [1]. In 2012, this w has been used in the IP-Glasma model [2] based on the color glass condensate (CGC) effective theory of QCD [3].

The inner structure of nucleons should also play a role in high-energy scattering. An effective partonic structure is introduced in Eq. (1) by introducing $T_A(\boldsymbol{x}) = \sum_{j=1}^{A_A} \sum_{q=1}^{n_c} \lambda_q g(x; \boldsymbol{x}_q, w_q)$, where for each nucleon, j, one samples the centers, $\boldsymbol{x}_q$, of n_c constituents from a Gaussian distribution of width w, and treats each sampled constituent as a Gaussian profile of width w_q. Incoherent production of J/Ψ in DIS probes the proton content fluctuations. In the CGC framework, one infers from data constituents of width $w_q \approx 0.10$ fm [4], albeit with a poor constraint on their number [5]. Three constituents of size 0.11 fm within nucleons of size 0.4 fm are currently implemented in IP-Glasma [6].

The second crucial ingredient for shaping the QGP is the energy deposition scheme, *i.e.*, a function of $T_A(\boldsymbol{x})$ and $T_B(\boldsymbol{x})$ that turns them into an energy density in the transverse plane, corresponding to the initial condition for the subsequent QGP formation. A robust prediction of the CGC framework is an average energy density of the form of $\langle T^{00}(\boldsymbol{x})\rangle[\mathrm{GeV/fm^3}] \propto Q_A^2(\boldsymbol{x})Q_B^2(\boldsymbol{x})$ [7]. The saturation scales, $Q^2_{A,B}$, involve the same function $T(\boldsymbol{b})$ appearing in the dipole cross section, and as such are essentially proportional to $T_{A,B}$[1]. The IP-Glasma model is based on such a scaling, as confirmed by comparisons with the IP-Jazma parametrization [8, 9]. Features of the CGC aside heavy-ion collision experiment point to a function of the kind $(T_A T_B)^\mu$ for the initial energy density. Note that the random normalizations of nucleons and constituents, *e.g.* λ_j in Eq. (1), affect less the QGP geometry compared to the widths w, w_q, or the energy deposition scheme, and will not be part of the present discussion.

2. 2015 — Entering the precision era

At the end of 2014, the Duke group devises a new Ansatz [10] for the entropy density at the beginning of the hydrodynamic phase of the QGP (TRENTo model)

$$\frac{\mathrm{d}S}{\mathrm{d}y}(\tau)\ \left[1/\mathrm{fm}^2\right] \equiv \tau s(\boldsymbol{x},\tau) \propto \left(\frac{T_A^p + T_B^p}{2}\right)^{1/p} . \tag{2}$$

Setting $p = 0$ leads to $\mathrm{d}S/\mathrm{d}y \propto \sqrt{T_A T_B}$, which is the only combination of the form of $(T_A T_B)^\mu$ that can result from Eq. (2). Let us reformulate this $p = 0$ model in a slightly different way. We introduce the energy density per unit rapidity at the initial time, and assume it is proportional to $(T_A T_B)^{2/3}$,

[1] Note that in TRENTo, the function T_A includes only the nucleons that participate in the collisions, whereas all nucleons are considered in the nuclear profiles in IP-Glasma.

$$\frac{\mathrm{d}E}{\mathrm{d}y}\left(\tau = 0^+\right)\ \left[\mathrm{GeV/fm^2}\right] \equiv \lim_{\tau\to 0^+} \tau e(\boldsymbol{x},\tau) \propto (T_A T_B)^{2/3}\ , \qquad (3)$$

where $e(\boldsymbol{x},\tau)$ is the energy density of the system in units GeV/fm^3. The initial $\mathrm{d}E/\mathrm{d}y$ can, then, be evolved (*e.g.*, freely streamed) to obtain the energy density at finite τ, $e(\boldsymbol{x},\tau)$. The latter retains the geometric features of the initial $\mathrm{d}E/\mathrm{d}y$. Upon application of the equation of state of high-temperature QCD, $s \propto e^{3/4}$, the resulting entropy per unit rapidity, $\mathrm{d}S/\mathrm{d}y$, will follow $(T_A T_B)^{2/3\times 3/4=1/2}$, as in the $p = 0$ Ansatz.

This model provides geometric features for the initial profiles that are close to those obtained within IP-Glasma. One example are the eccentricities, ε_n, which are the seeds of the anisotropic flow, v_n. The TRENTo prescription allows one, thus, to produce results of potentially similar quality as those obtained in IP-Glasma within a simpler framework. The possibility of mass-producing millions of TRENTo initial conditions opens a new way to compare initial-state calculations to data, and investigate observables that are too costly for hydrodynamic simulations [11]. Thanks to TRENTo, the soft sector of heavy-ion collisions enters a new era of precision.

3. 2016 — The first Bayesian analysis

In 2016, the Duke group performs the first Bayesian analysis (hereafter referred to as Duke-16) of 2.76 TeV Pb+Pb data [12]. The analysis aims at the inference of high-probability (or Maximum A Posteriori, MAP) parameters for the initial state and the transport properties of the QGP. The TRENTo model is used as an entropy density at the beginning of hydrodynamics ($\tau = 0.4$ fm/c). The analysis is very successful. A notable result is the posterior distribution of the generalized mean parameter, p, which is strongly peaked around $p = 0$, confirming an initial geometry in agreement with that of IP-Glasma. Another important result concerns the nucleon size. The prior range for this parameter is between 0.4 fm and 1 fm. The MAP value is around $w = 0.45$ fm, meaning that data gives a strong preference for a small size. Remarkably, then, both analyses of diffractive J/Ψ production at HERA and a Bayesian analysis of heavy-ion collisions based on the TRENTo model return nucleons of the same size. As of 2016, the energy deposition is essentially $\mathrm{d}E/\mathrm{d}y(\tau = 0^+) \propto (T_A T_B)^{2/3}$, with $w = 0.45$ fm. See Fig. 1.

4. 2019/2020 — Prescription changes and nucleons swell

Things take a dramatic turn with a new Bayesian analysis of the Duke group (Duke-19) [13], inferring more parameters from data (*e.g.*, the temperature dependence of the specific bulk viscosity, ζ/s), and including a free-streaming pre-hydrodynamic phase. The TRENTo model becomes the initial condition for this free streaming phase and plays the role of the energy

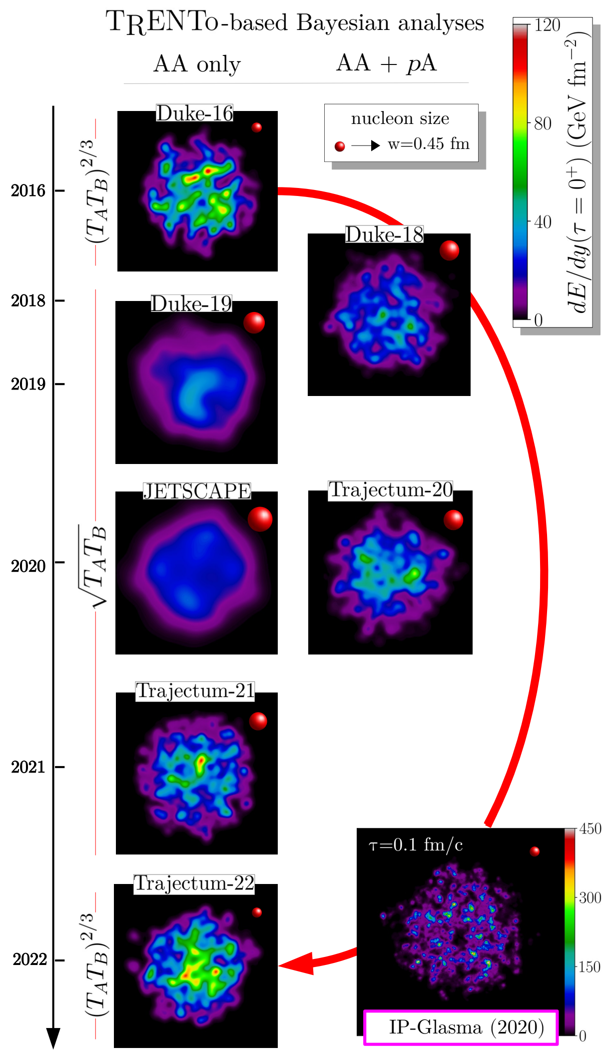

Fig. 1. Circle trip of the initial energy density per unit rapidity, dE/dy, and of the nucleon size, w, in initial-state parametrizations inferred from Bayesian analyses of nucleus–nucleus and proton–nucleus collisions in the past six years. Each plot shows one Pb+Pb collision at $b = 0$ and $\sqrt{s_{NN}} = 2.76$ TeV. Each profile in the (x, y) plane is plotted in the square $-10 \leq x \leq 10$ fm, $-10 \leq y \leq 10$ fm.

density per unit rapidity, dE/dy. The found MAP value of p remains $p = 0$, *i.e.*, the only allowed combination of the type $(T_AT_B)^{\mu}$. The global analysis provides an excellent description of the considered experimental data, though one issue arises. The nucleon size, still constrained from a prior range $w \in [0.4, 1]$ fm, acquires a MAP value $w = 0.96$ fm, doubling the 2016 estimate. The combined effect of this large nucleon size and switching from $\mathrm{d}S/\mathrm{d}y$ to $\mathrm{d}E/\mathrm{d}y$ at the same value of p leads to extremely smooth initial conditions for the QGP, as shown in Fig. 1. This result has been found as well in 2020 by the JETSCAPE Collaboration in their analysis of Pb+Pb and Au+Au data [14]. Figure 1 shows, in particular, the JETSCAPE initial condition obtained with so-called Grad-type viscous corrections at freeze-out, where the MAP width is $w = 1.12$ fm. A consequence of these smooth profiles is the damping of pressure gradients in the fluid, which in turn require much reduced ζ/s ($(\zeta/s)_{\max} \approx 0.03$ in Duke-19, while $(\zeta/s)_{\max} \approx 0.1$ with IP-Glasma initial conditions) to reproduce the measured radial flow. Similar results have been obtained as well in the recent analysis of Parkkila *et al.* [15, 16] ($w \approx 0.8$ fm). We remark, then, that the latest version of the IP-Glasma model of the initial condition also appears in 2020 [6]. As shown in Fig. 1, the predicted initial profile is sharp and lumpy, due to the fine nucleon structure. At the end of 2020, IP-Glasma and T_RENTo models based on Bayesian analyses of nucleus–nucleus data are starkly inconsistent, both in terms of initial profiles and in terms of implemented bulk viscosities.

Let us comment, then, on the Bayesian analysis of Ref. [17] (Duke-18) using the same model as in Duke-19, albeit including experimental data from proton–nucleus collisions. Following the implementation of the nucleon sub-structure in IP-Glasma [18], the Duke-18 calculation introduces nucleon constituents to make the T$_\mathrm{R}$ENTo Ansatz viable for small systems. Remarkably, the $p = 0$ Ansatz remains the only viable model as well when p+Pb data is included. This is probably driven by the A–A data, as it is not known at present whether analyzing p–A alone would give the same result. Similar results are obtained as well in the first Bayesian analysis within the Trajectum framework (Trajectum-20) [19]. Both Duke-18 and Trajectum-20 infer rather large nucleon sizes, $w \approx 0.9$ fm, though with a constituent size $w_q \approx 0.5$ fm. Comparing, then, these profiles with the JETSCAPE and Duke-19 ones in Fig. 1, we can see the presence of short-range structures coming from the nucleon constituents. These additional structures do not imply larger values of ζ/s, which remain very close to zero [19].

5. 2021/2022 — Deflating the quark–gluon plasma via ζ/s

The profiles of Duke-19 or JETSCAPE are clearly questionable. There is no apparent issue with an initial energy density of the form $(T_A T_B)^{1/2}$, but the too large size of nucleons seems problematic. Although we may not fully understand why experimental data tends to favor such smooth profiles, it may be possible to find observables that depend in a dramatic way on the nucleon size, allowing us to stress-test these results. One such observable is the Pearson correlation between the charged-hadron mean transverse momentum, $\langle p_\mathrm{T}\rangle$, and anisotropic flow, v_n^2, denoted by $\rho(\langle p_\mathrm{T}\rangle, v_n^2)$ [20].

As emphasized by the ALICE Collaboration [21], this correlator presents a unique model dependence. For instance, $\rho(v_3^2, \langle p_{\mathrm{T}}\rangle)$ is negative at almost all centralities in the JETSCAPE results, while it is positive with IP-Glasma initial conditions, in agreement with experimental measurements [21–23]. This largely comes from the huge difference in the implemented size of nucleons [24]. Even the model outcome of the sophisticated Bayesian analysis performed in 2021 within the Trajectum framework (Trajectum-21) by Nijs and van der Schee [25], with the well-structured initial profile shown in Fig. 1, yields hydrodynamic results for $\rho(v_n^2, \langle p_{\mathrm{T}}\rangle)$ that are inconsistent with data [23]. The reason is partly that the nucleon size remains too large, ≈ 0.85 fm.

One way to fix this issue is to look at the total inelastic nucleus–nucleus cross section, σ_{AA}. In T_RENTo and IP-Glasma, the nucleon size determines the probability of interaction between two ions at a given impact parameter. The cross section is constrained fairly well by Glauber fits of multiplicity distributions [26], and provides an experimental handle on w. The latest Trajectum study (Trajectum-22) [27] enforces the Bayesian analysis to return a reasonable value of σ_{AA}. Doing so, not only the nucleon size shrinks to a value close to 0.5 fm, but the exploration of a doubly-generalized average with an additional parameter, q, $\frac{\mathrm{d}E}{\mathrm{d}y}(\tau = 0^+) \propto \left(\frac{T_A^p + T_B^p}{2}\right)^{q/p}$, shows that, when the σ_{AA} constraint is properly considered (and the computed $\rho(v_n^2, \langle p_{\mathrm{T}}\rangle)$ correlators are qualitatively consistent with data), the favored initial-state model has $q \approx 4/3$ and $p \approx 0$, *i.e.*, $\mathrm{d}E/\mathrm{d}y \propto (T_B T_B)^{2/3}$ [28]. The circle is closed (see Fig. 1). We are back to the nucleon size and energy deposition of Duke-16 (albeit with four constituents per nucleon, and $w_q \approx 0.4$ fm). We stress that these sharper profiles now impact visibly the extracted $\zeta/s(T)$, whose maximum increases by a large factor [27].

6. What now?

Recapping, as of 2022, the state-of-the-art modeling of the quark–gluon plasma returned by Bayesian analyses contains an initial $\mathrm{d}E/\mathrm{d}y$ that scales like $(T_A T_B)^{2/3}$, with a nucleon size $w \approx 0.5$ fm, and 3–4 constituents per nucleon having $w_q \approx 0.4$ fm. It is yet to be understood how this model is connected to IP-Glasma, although their predictions appear to be reasonably consistent. To improve the state-of-the-art, one may include in future Bayesian analyses selected multi-particle correlation observables that offer a stronger sensitivity to the initial condition. Natural candidates are the $\rho(v_n^2, \langle p_{\mathrm{T}}\rangle)$ correlators, though much insight would come as well from the relative fluctuation of v_3, $v_3\{4\}/v_3\{2\}$, or the skewness of the fluctuations of $\langle p_{\mathrm{T}}\rangle$ [11, 29]. At the price of increasing dramatically the computational effort, these observable would indeed permit global analyses to yield tighter constraints on the initial-state properties.

It would be desirable, in addition, to clarify the fundamental origin of the dependence of observables on model features. This may be achieved via a model-independent description of the initial states in terms of correlation functions of fluctuating fields. Techniques to do so have been discussed in the past [30, 31]. Does $\rho(v_n^2, [p_\mathrm{T}])$ depend on the nucleon size because the latter modifies the local average of the energy density field, or because it modifies the local variance? What is the main difference between implementing $w_q = 0.4$ fm as in Trajectum-22 and $w_q = 0.11$ fm as in IP-Glasma? Is it in the local variance of the density field, or in its correlation length?

Features of the ^{208}Pb nucleus itself should also be included in future Bayesian analyses. Introducing a nuclear skin thickness parameter would be especially interesting, as this feature affects σ_{AA} and the sharpness of the average density profiles. The nucleon density in a nucleus, ρ_m, can be written as $\rho_m = \rho_p + \rho_n$, where $\rho_{n(p)}$ is the density of neutrons (protons). While ρ_p is known from low-energy experiments, ρ_n, and in particular its skin, is not. One could attempt, thus, at inferring the neutron density of ^{208}Pb via the Bayesian analysis of high-energy data. This would in turn provide an independent estimate of the neutron skin of this nucleus, a hot topic in low-energy nuclear physics due to its relevance for the understanding of the properties of neutron stars [32, 33].

The author expresses his gratitude to all the colleagues who across the year 2021 have helped make progress on the issue of the nucleon size in the results of Bayesian analyses. I acknowledge in particular Bjoern Schenke, Chun Shen, Wilke van der Schee, Govert Nijs, Matt Luzum, Jean-Yves Ollitrault, Jamie Nagle, Jiangyong Jia, and You Zhou for fruitful discussions on this matter. This research work is funded by the Deutsche Forschungsgemeinschaft (DFG, German Research Foundation) under Germany's Excellence Strategy EXC2181/1-390900948 (the Heidelberg STRUCTURES Excellence Cluster), within the Collaborative Research Center SFB1225 (ISOQUANT, Project-ID 273811115).

REFERENCES

[1] A. Caldwell, H. Kowalski, *Phys. Rev. C* **81**, 025203 (2010).

[2] B. Schenke, P. Tribedy, R. Venugopalan, *Phys. Rev. Lett.* **108**, 252301 (2012).

[3] F. Gelis, E. Iancu, J. Jalilian-Marian, R. Venugopalan, *Annu. Rev. Nucl. Part. Sci.* **60**, 463 (2010).

[4] H. Mäntysaari, B. Schenke, *Phys. Rev. Lett.* **117**, 052301 (2016)

[5] H. Mäntysaari, B. Schenke, C. Shen, W. Zhao, *Phys. Lett. B* **833**, 137348 (2022).

[6] B. Schenke, C. Shen, P. Tribedy, *Phys. Rev. C* **102**, 044905 (2020).

[7] F. Gelis, «Quantum Field Theory», *Cambridge University Press*, 2019.

[8] J.L. Nagle, W.A. Zajc, *Phys. Rev. C* **99**, 054908 (2019).

[9] R. Snyder, M. Byres, S.H. Lim, J.L. Nagle, *Phys. Rev. C* **103**, 024906 (2021).

[10] J.S. Moreland, J.E. Bernhard, S.A. Bass, *Phys. Rev. C* **92**, 011901 (2015).

[11] G. Giacalone, J. Noronha-Hostler, J.Y. Ollitrault, *Phys. Rev. C* **95**, 054910 (2017).

[12] J.E. Bernhard *et al.*, *Phys. Rev. C* **94**, 024907 (2016).

[13] J.E. Bernhard, J.S. Moreland, S.A. Bass, *Nature Phys.* **15**, 1113 (2019).

[14] JETSCAPE Collaboration (D. Everett *et al.*), *Phys. Rev. C* **103**, 054904 (2021).

[15] J.E. Parkkila, A. Onnerstad, D.J. Kim, *Phys. Rev. C* **104**, 054904 (2021).

[16] J.E. Parkkila *et al.*, *Phys. Lett. B* **835**, 137485 (2022), `arXiv:2111.08145 [hep-ph]`.

[17] J.S. Moreland, J.E. Bernhard, S.A. Bass, *Phys. Rev. C* **101**, 024911 (2020).

[18] H. Mäntysaari, B. Schenke, C. Shen, P. Tribedy, *Phys. Lett. B* **772**, 681 (2017).

[19] G. Nijs, W. van der Schee, U. Gürsoy, R. Snellings, *Phys. Rev. Lett.* **126**, 202301 (2021).

[20] P. Bozek, *Phys. Rev. C* **93**, 044908 (2016).

[21] ALICE Collaboration (S. Acharya *et al.*), *Phys. Lett. B* **834**, 137393 (2022), `arXiv:2111.06106 [nucl-ex]`.

[22] ATLAS Collaboration (G. Aad *et al.*), *Eur. Phys. J. C* **79**, 985 (2019).

[23] ATLAS Collaboration, `arXiv:2205.00039 [nucl-ex]`.

[24] G. Giacalone, B. Schenke, C. Shen, *Phys. Rev. Lett.* **128**, 042301 (2022).

[25] G. Nijs, W. van der Schee, `arXiv:2110.13153 [nucl-th]`.

[26] ALICE Collaboration, `arXiv:2204.10148 [nucl-ex]`.

[27] G. Nijs, W. van der Schee, `arXiv:2206.13522 [nucl-th]`.

[28] G. Nijs, W. van der Schee, to appear.

[29] G. Giacalone, F.G. Gardim, J. Noronha-Hostler, J.Y. Ollitrault, *Phys. Rev. C* **103**, 024910 (2021).

[30] S. Floerchinger, U.A. Wiedemann, *Phys. Lett. B* **728**, 407 (2014).

[31] J.P. Blaizot, W. Broniowski, J.Y. Ollitrault, *Phys. Lett. B* **738**, 166 (2014).

[32] PREX Collaboration (D. Adhikari *et al.*), *Phys. Rev. Lett.* **126**, 172502 (2021).

[33] B.T. Reed, F.J. Fattoyev, C.J. Horowitz, J. Piekarewicz, *Phys. Rev. Lett.* **126**, 172503 (2021).